

# Local texture and percolative paths for long-range conduction in high critical current density $\text{TlBa}_2\text{Ca}_2\text{Cu}_3\text{O}_{8+x}$ deposits

D. M. Kroeger, A. Goyal, E. D. Specht, and Z. L. Wang  
Oak Ridge National Laboratory, P. O. Box 2008, Oak Ridge, Tennessee 37831

J. E. Tkaczyk, J. A. Sutliff, and J. A. DeLuca  
General Electric Corporate R&D, P. O. Box 8, Schenectady, New York 12301

(Received 12 July 1993; accepted for publication 25 October 1993)

A possible microstructural origin of the high critical current densities which have been obtained in *c*-axis-aligned, polycrystalline  $\text{TlBa}_2\text{Ca}_2\text{Cu}_3\text{O}_{8+x}$  deposits has been identified. The results of x-ray diffraction determinations of basal plane texture of Tl-1223 deposits prepared by spray pyrolysis are observed to depend on the size of the x-ray beam. Furthermore, most grain boundaries were found from transmission electron microscopy to have small misorientation angles. It is concluded that although overall the basal plane orientations are nearly random, there is a high degree of local texture indicative of colonies of similarly oriented grains. The spread in *a*-axis orientation within a colony is  $\sim 10^\circ$ – $15^\circ$ . Intercolony conduction, it is suggested, may be enhanced by a percolative network of small-angle grain boundaries at colony interfaces.

Recent studies have shown that spray-pyrolyzed films of the Tl-1223 compound ( $\text{Tl}_x\text{Ba}_2\text{Ca}_2\text{Cu}_3\text{O}_y$ , with  $0.7 < x < .95$ ) on polycrystalline yttria-stabilized zirconia substrates can be prepared which have  $J_c$  near  $10^5$  A/cm<sup>2</sup> at 77 K, in zero field.<sup>1,2</sup> The films are polycrystalline and have excellent *c*-axis alignment (rocking curve full width at half maximum  $\sim 2^\circ$ ). Electron backscatter diffraction (EBSD) patterns obtained from widely separated regions on the films indicate lack of macroscopic in-plane texture.<sup>3</sup> Nevertheless, the films show little evidence of weak-link behavior. The  $J_c$ -vs- $H$  curve for ( $H \parallel c$ ) has a plateau extending to 1 T at 77 K.<sup>1-3</sup> Furthermore, recent studies on similar films containing columnar defects resulting from irradiation with Ag ions have shown that under conditions of optimal defect densities the irreversibility field at 77 K is in the range reported for  $\text{YBa}_2\text{Cu}_3\text{O}_7$  (Y123).<sup>4</sup> These results indicate the enormous potential of Tl-1223 thick films for high-temperature, high-field applications. It is therefore important to determine the nature of grain boundaries and understand the mechanism responsible for non-weak-link current flow in these films. Preliminary results of microstructural studies addressing these critical issues are reported here.

Samples were prepared according to procedures described previously.<sup>2</sup> Film thicknesses were approximately 3  $\mu\text{m}$ . Zero-field  $J_c$ 's at 77 K were measured with an electric field criterion of 1  $\mu\text{V}/\text{cm}$  on a bridge pattern etched from the film. The bridge dimensions were  $4 \times 0.2$  mm. There were five voltage connections, one at each of the current tabs and three at 1-mm intervals along the bridge (points A–E of the inset in Fig. 3), permitting measurement of  $J_c$  in each of four 1-mm segments. As described previously,<sup>2</sup>  $J_c$  varies by as much as a factor of 3 or 4 from segment to segment. Microstructural information regarding grain morphology and grain boundary chemistry and misorientation was obtained using scanning and transmission electron microscopy (SEM and TEM). Local texture information was inferred from x-ray diffraction (XRD) measurements and TEM.

Results of basal plane texture determinations from XRD

azimuthal scans were found to depend on the size of the x-ray beam, indicating the presence of local texture in deposits which overall appear to be nearly untextured. Figure 1 shows two XRD azimuthal scans of the same deposit. The positions of source and detector and the axis of rotation of the sample are indicated. The detector was positioned to detect a non-(00 $l$ ) peak. Since the deposit has good *c*-axis alignment the intensity at a given angle  $\phi$  is proportional to the fraction of the deposit area illuminated by the beam which had some specific basal plane orientation. Thus, the  $\phi$  scans of Fig. 1 are, effectively, distribution plots for the directions of the *a* axes of grains relative to a fixed arbitrary angle. Figure 1(a) indicates the intensity of the (103) reflection as a function of rotation about the film normal (i.e., the

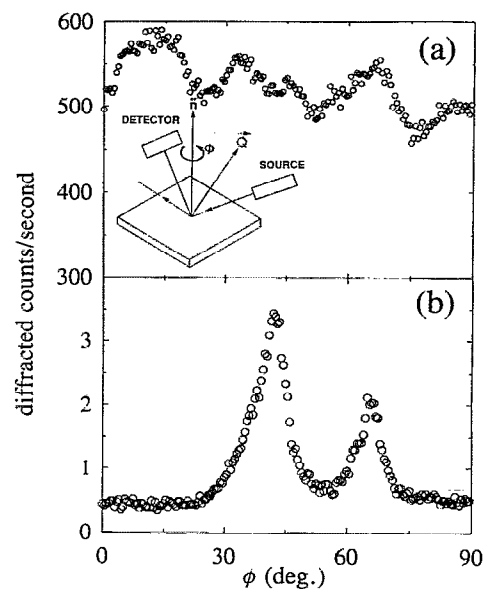


FIG. 1. Intensity distributions for x-ray diffraction azimuthal scans using (a) wide and (b) narrow x-ray beams.



FIG. 2. TEM cross-section image showing the substrate, a thin reaction layer, and tilt (perpendicular to the substrate) and twist (parallel to the substrate) grain boundaries. As indicated by the arrows, tilt boundaries tend, in combination with short segments of twist boundary, to extend over several grains. The thin area in this view covers about half the sample thickness.

*c* axis). The data were obtained using a wide x-ray beam sufficient to illuminate all or most of the area of a current tab ( $4 \times 8$  mm). The intensity distribution consists of several peaks superimposed on an average intensity which is well above background. These data suggest that basal plane orientations of grains are largely random, but that there is a tendency for clustering about several specific directions. This result is consistent with previous EBSD measurements of the orientations of a large number of grains at random locations. However, a very different intensity distribution was obtained when a narrow x-ray beam was used, indicating that locally grains are far from randomly oriented. Figure 1(b) shows an azimuthal scan of the  $(10\bar{1}0)$  reflection obtained with a narrow beam which had a projected area on the sample of  $\sim 0.5 \times 1$  mm. The intensity distribution shows two strong peaks with a low intensity (near background) at all other angles, indicating that basal plane orientations for grains within the illuminated area cluster strongly about only two directions. For approximately 20 such local scans obtained on separate areas of two different deposits, the number of peaks ranged from 1 to 5. These results indicate that, although over the whole deposit many basal plane orientations occur, there is a high degree of local texture indicative of the presence of colonies of grains with similar orientations.

Figure 2 shows a TEM image of a cross-section specimen in which both twist boundaries (parallel to the basal plane) and tilt boundaries (approximately perpendicular to the basal plane) are seen. Alignment of the *c* axis perpendicular to the substrate surface is seen to be good. Misorientation angles of 20 grain boundaries, 11 twist and 9 tilt, have been measured from convergent-beam electron diffraction. Ten of the twist boundaries had misorientation angles less than  $10^\circ$  and five of the tilt boundaries had misorientation

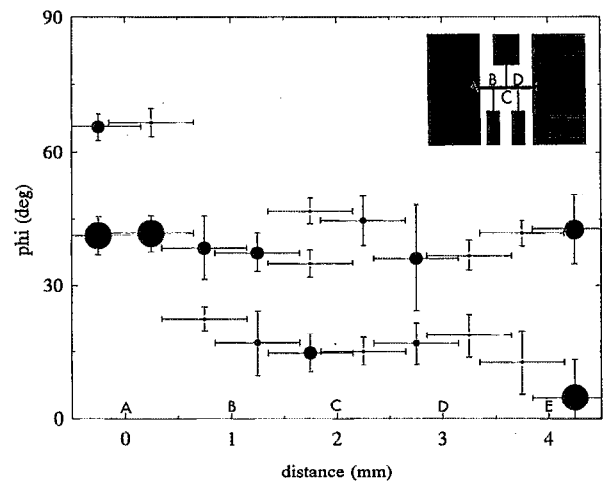


FIG. 3. Angular positions of peaks in x-ray diffraction azimuthal scan intensity distributions obtained using a narrow beam [as in Fig. 1(b)] as a function of position along the gauge length. The bridge length A–E (see inset) is 4 mm and the segments A–B, B–C, etc., are 1 mm. The current pads are  $4 \times 8$  mm. The size of the symbol indicates peak intensity, vertical bars indicate the peak's FWHM, and horizontal bars indicate the dimension (1 mm) of the beam, and thus the overlap of area sampled. The zero-field critical current densities of the various segments are  $AB = 44\,118$  A/cm<sup>2</sup>,  $BC = 18\,873$  A/cm<sup>2</sup>,  $CD = 88\,235$  A/cm<sup>2</sup>, and  $DE = 85\,784$  A/cm<sup>2</sup>.

angles under  $15^\circ$ . Nearly all grain boundaries are clean, in the sense that secondary phases are absent. However, composition determinations at edge-on twist boundaries from energy dispersive electron spectroscopy indicate thallium enrichment compared to the bulk. High-resolution images suggest that this nonstoichiometry results from the nature of the grain termination at the boundary rather than a grain boundary phase. Thallium enrichment at *c*-axis twist boundaries is significantly enhanced by a post-thallination treatment in oxygen at  $600^\circ\text{C}$  which has been found to increase the  $J_c$ . These results will be discussed in detail in a subsequent paper.

SEM images of fracture surfaces and EBSD measurements of basal plane orientations indicate that basal plane dimensions of grains are in the range of 3 to  $10\ \mu\text{m}$ . TEM images indicate that in the *c* direction grain thicknesses tend to range from 0.5 to  $2\ \mu\text{m}$ . Aspect ratios are thus  $\sim 10$ , intermediate between those in Y123 and Bi-Sr-Ca-Cu-O. The average thickness of the deposit is  $\sim 3\ \mu\text{m}$ , so that in most areas it is only a few grains thick. Examination of a number of images suggests that perpendicular boundaries tend, in association with short segments of parallel boundaries, to extend through the thickness of the deposit (see the arrows in Fig. 2).

Figure 3 summarizes the results of a series of azimuthal XRD scans taken at 0.5-mm intervals along the 4-mm-long gauge length of a patterned specimen. The angular positions of XRD peaks from plots obtained using a narrow beam, as in Fig. 1(b), are plotted as a function of position along the gauge length. The measured  $J_c$ 's for each of the four sections are indicated. The projected area of the x-ray beam is approximately  $0.5 \times 1$  mm, so there is substantial overlap of areas sampled for adjacent measurements, as indicated by the horizontal bars. Vertical bars indicate the full width at half-

maximum (FWHM) of the peaks, and thus are a measure of the spread in  $a$ -axis orientations. The size of the circle indicates peak intensity, which was influenced not only by the relative number of grains with that orientation, but also by the amount of deposit area sampled, as determined by proximity to current and voltage tabs. The number of  $a$ -axis orientations varied from 1 to 3 over the gauge length. Although particular  $a$ -axis orientations, presumably indicative of colonies of grains of similar orientation, arise and disappear as a function of position, it appears that there is usually a small-angle boundary connection between adjacent areas. The results for this particular sample suggest that within the gauge length there may be only three colonies, one of which extends over the whole length. Alternatively, there may be a larger number of colonies, with a tendency for colony orientations to be correlated locally. Results on a second sample suggest, however, that this tendency for continuity of orientation over distance may not be general. Further experiments are in progress. The spread in grain orientations within a colony increases the likelihood that at least some of the boundaries between grains in adjacent areas will be small angle. It is possible that non-weak-linked intercolony flow is through such boundaries. Since the Tl-1223 compound is tetragonal, the largest misorientation angle for boundaries between  $c$ -axis-aligned grains is  $45^\circ$ .

Within a colony, since most grain boundaries have small misorientations, current flow should not be weak-linked. Two possible modes for non-weak-linked intercolony current flow may be envisioned. First is a percolative path of "good" tilt boundaries at colony boundaries. These good boundaries may be small-angle tilt boundaries which, as discussed above, are likely to occur because of the spread in grain orientations within a colony, or they may be low-energy (i.e., low  $\Sigma$ ) boundaries. The probability of small-angle boundaries at colony intersections increases with the spread in grain orientations within a colony. A local bias in colony orientations resulting in a tendency for adjacent colonies to have similar orientations, as the results in Fig. 3 may suggest, would increase the number of small-angle boundaries. Second, current flow through  $c$ -axis twist boundaries between overlapping grains at colony intersections, which may have larger area than the tilt boundaries, may be significant. However, the observed increase in nonstoichiometry (Tl-rich, Ca-poor) at twist boundaries which we find accompanies the increase in  $J_c$  resulting from treatment at  $600^\circ\text{C}$  in  $\text{O}_2$  casts doubt on this mode of intercolony current transfer. We also note that grain aspect ratios are not large, and typical

TEM images of tilt boundaries, as in Fig. 2, do not suggest that the area for  $c$ -axis conduction around tilt boundaries is large compared to the tilt boundary area. Conduction in the  $c$  direction through  $c$ -axis twist grain boundaries is an essential component of the brick-wall model<sup>5-7</sup> which has been widely discussed<sup>7-9</sup> as an explanation of non-weak-linked current flow in  $c$ -axis-aligned polycrystalline materials, such as Bi-based powder-in-tube conductors. The most significant objection to the model arises from the temperature dependence of the critical current density, which has been found to match that for basal plane conduction,<sup>10</sup> suggesting that  $c$ -axis conduction does not play a significant role in long-range transport. The present work indicates that in  $c$ -axis-aligned polycrystalline materials local in-plane texture can lead to a percolative path of strongly linked  $c$ -axis tilt grain boundaries which appear to make  $c$ -axis conduction unnecessary. Present knowledge of the more complicated microstructures encountered in Bi-based powder-in-tube conductors is insufficient to determine if a similar condition exists in those materials.

We would like to thank D. K. Christen and V. Selvamanickam for valuable comments, and Gwen Sims for preparation of the manuscript. This research was sponsored by the U. S. Department of Energy Office of Advanced Utility Concepts—Superconducting Technology Program under Contract No. DE-AC05-84OR21400 with Martin Marietta Energy Systems, Inc.

- <sup>1</sup>J. E. Tkaczyk, J. A. DeLuca, P. L. Karas, P. J. Bednarczyk, M. F. Garbaskas, R. H. Arendt, K. W. Lay, and J. S. Moodera, *Appl. Phys. Lett.* **61**, 610 (1992).
- <sup>2</sup>J. A. DeLuca, P. L. Karas, J. E. Tkaczyk, P. J. Bednarczyk, M. F. Garbaskas, C. L. Briant, and D. B. Sorensen, *Physica C* **205**, 21 (1993).
- <sup>3</sup>D. J. Miller, J. G. Hu, J. D. Hettlinger, K. E. Gray, J. E. Tkaczyk, J. A. DeLuca, P. L. Karas, J. A. Sutliff, and M. F. Garbaskas, *Appl. Phys. Lett.* **62**, 3031 (1993).
- <sup>4</sup>J. E. Tkaczyk, J. A. DeLuca, P. L. Karas, P. J. Bednarczyk, D. K. Christen, C. E. Klabunde, and H. R. Kerchner, *Appl. Phys. Lett.* **62**, 3031 (1993).
- <sup>5</sup>J. Mannhart and C. C. Tsuei, *Z. Phys. B* **77**, 53 (1989).
- <sup>6</sup>A. P. Malozemoff, in *High Transition Temperature Compounds II*, edited by S. H. Whang, A. DasGupta, and R. B. Laikowitz (TMS, Warrendale, PA, 1990), p. 3.
- <sup>7</sup>L. N. Bulaevskii, J. R. Clem, L. I. Glazman, and A. P. Malozemoff, *Phys. Rev. B* **45**, 2545 (1992).
- <sup>8</sup>L. N. Bulaevskii, L. L. Daemen, M. P. Maley, and J. Y. Coulter, *Phys. Rev. B* (to be published).
- <sup>9</sup>A. Umezawa, Y. Feng, H. S. Edelman, Y. E. High, D. C. Larbalestier, Y. S. Sung, and E. E. Hellstrom, *Physica C* **198**, 261 (1992).
- <sup>10</sup>B. Hensel, J.-C. Grivel, A. Jeremie, A. Perin, A. Pollini, and R. Flükiger, *Physica C* **205**, 329 (1993).